Bioorganic Chemistry 89 (2019) 103035

Contents lists available at ScienceDirect

Bioorganic Chemistry

journal homepage: www.elsevier.com/locate/bioorg

Design, synthesis and anticervical cancer activity of new benzofuran–pyrazol-hydrazono- thiazolidin-4-one hybrids as potential EGFR inhibitors and apoptosis inducing agents

Hebat-Allah S. Abbas[a,b], Somaia S. Abd El-Karim[c,*]

[a] Chemistry Department, College of Science, King Khalid University, Abha, Saudi Arabia
[b] Photochemistry Department, National Research Centre, Dokki, Cairo 12622, Egypt
[c] Department of Therapeutic Chemistry, National Research Centre, Dokki, Cairo 12622, Egypt

ARTICLE INFO

Keywords:
Benzofuran
Pyrazole
Thiazolidin-4-one
Cervical cancer
Apoptosis and EGFR PK suppressing agents

ABSTRACT

This study represents the synthetic approaches of a new set of 2-(((3-(benzofuran-2-yl)-1-phenyl-1*H*-pyrazol-4-yl)methylene)hydrazono)-5-(aryl)thiazolidin-4-one derivatives **4–22** aiming to obtain new antiproliferative candidates against human cervix carcinoma cells (Hela) of EGFR PK inhibiting potency. The cancer cells represented promising sensitivity towards the compounds **6**, **7**, **11**, **13**, **14**, **16**, **17** more than or equal to that against the reference drug doxorubicin. In addition, the latter compounds were tested as EGFR protein kinase inhibitors. The results revealed that compound **14** showed more significant EGFR PK inhibitory activity than the reference drug erlotinib (IC50; 0.07, 0.08 μM, respectively). Moreover, cell cycle analysis and apoptosis assay were performed for compound **14** proving its ability to cause G1/S phase arrest and apoptosis in Hela cancer cells, in addition to its activation of the caspases-7 and -3. In addition, derivative **14** increased the expression level of p53 and the ratio of Bax/Bcl-2 which confirmed its mode of action. Molecular docking study of **14** was performed to investigate its binding mode of interaction with EGFR PK in the active site with the aim of rationalizing its promising inhibitory activity. Accordingly, compound **14** might be considered as a promising scaffold anticervical cancer chemotherapeutic and deserves further optimization and in-depth biological studies.

1. Introduction

Cancer disease is a life-threatening disease and its treatment is a significant challenge over the past 100 years [1]. It has been documented that the organs; liver, prostate, lung, stomach and colorectal are mostly affected by cancer disease in men, whereas among women, breast, cervix, thyroid, colorectal and lung are the mostly affected by cancer [2], where the cervical cancer is considered the fourth most frequent cancer among women with an estimated 570,000 new cases in 2018 representing 6.6% of all female cancers [3]. Approximately ninety percent of deaths which occur as a result of cervical cancer appear in low- and middle-income countries [3]. Although the majority of women present with early-stage disease and can be treated successfully, 25% of women are present with advanced disease. Tremendous efforts are still needed to improve the overall survival rate in patients with advanced-stage cervical cancer in addition to the discovery of new drugs that have selectivity to inhibit the growth of the tumor cells or completely kill them without producing toxic effects on the healthy cells [2,3].

Receptor protein tyrosine kinases (PTKs) play crucial roles in activating signal transduction pathways in the cells, resulting in cell division, differentiation, and regulatory mechanisms. Epidermal growth factor receptor (EGFR) kinase is a receptor tyrosine kinase (RTK) of the ErbB family [4]. It regulates numerous biological pathways, such as; cell motility, adhesion, and cell cycle regulation, as well as angiogenesis, apoptosis, and metastasis [5,6]. Over-expression of EGFR PK is also crucial for the evolution of malignant tumors, such as colon, ovarian, breast and non-small cell lung cancer (NSCLC) [7]. Fig. 1 represents various approved anticancer drugs targeting inhibition of EGFR kinase [8–12].

It has been reported that, oxygen bearing heterocyclic rings reveal an eminent class of compounds displaying interesting biological activities, due to their similarity to various natural bioactive molecules [13]. Benzofurans have the ability to inhibit particular serine/threonine kinases whose deregulation is correlated with cancer development, and reduce the proliferation of different tumor cells such as cervical and liver cancer cells by stopping the cycle of the cell at G2/M phase

* Corresponding author.
E-mail address: somaia_elkarim@hotmail.com (S.S. Abd El-Karim).

https://doi.org/10.1016/j.bioorg.2019.103035
Received 21 March 2019; Received in revised form 23 May 2019; Accepted 3 June 2019
Available online 04 June 2019

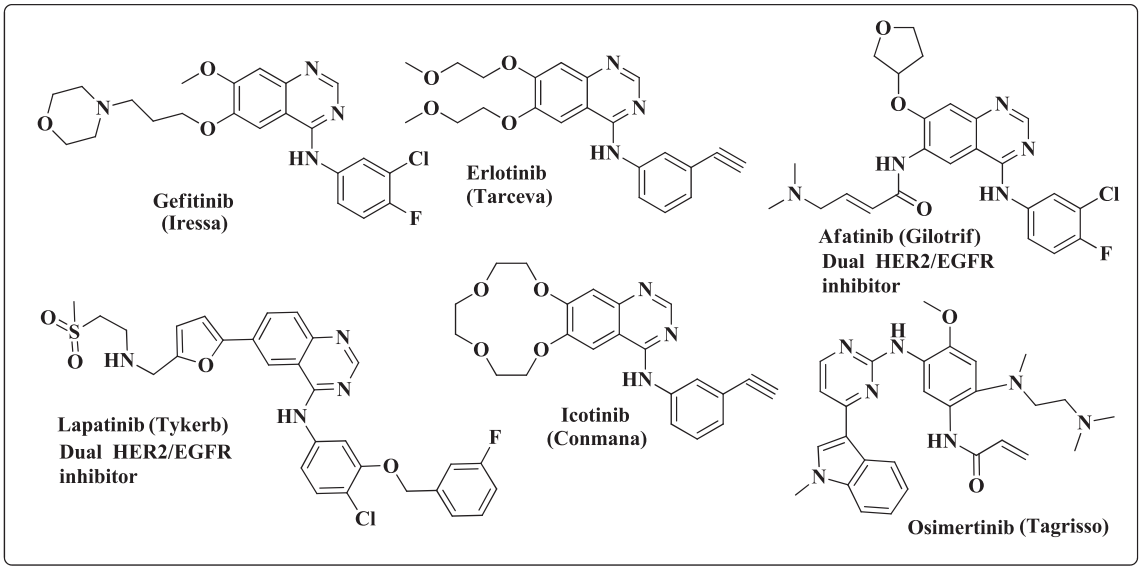

Fig. 1. Drugs of EGFR PK inhibiting activity.

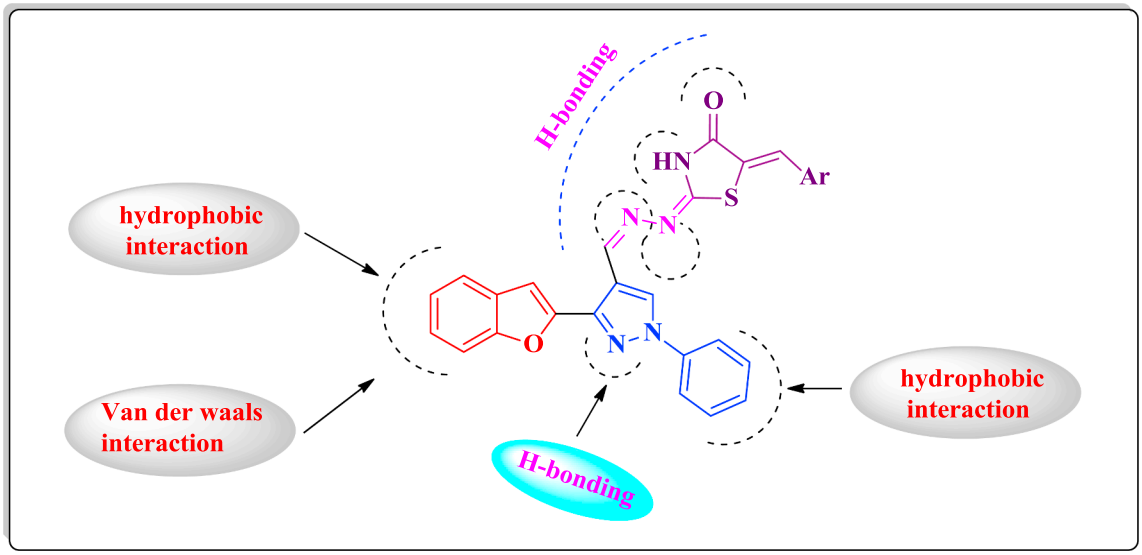

Fig. 2. Proposed hypothetic model for the new benzofuran-pyrazole-thiazolidinone compounds.

[13,14]. In addition, different compounds carrying the pyrazole skeleton were reported as potent anticancer agents inducing strong apoptosis and cell cycle arrest in addition to effective EGFR tyrosine kinase suppression of inhibiting IC50 values reaching single digit nanomolar range [15]. Moreover, the hydrazone functional groups were reported to optimize the anticancer potency of different compounds inducing anticancer activity [16]. Furthermore, thiazole and thiazolidine pharmacophores occupy an important place in the field of anticancer chemotherapy targeting different proteins [17,18]. Due to the appearance of intrinsic resistance and an insufficient response towards many effective anticancer drugs [19] and the hope to generate new more effective and selective anticancer agents, the scope of the design of the new derivatives in this study was based on hybridization of benzofuran-pyrazole core with substituted thiazolidinone moieties via a hydrazone linkage aiming to gain a new scaffold for the synthesis of novel antiproliferative agents of synergistic activity. The impact of molecular orientation, ring size variance and heteroatoms existence which could participate in the interaction with EGFR PK binding pocket via hydrogen bonding were taken in consideration (Fig. 2). The newly synthesized target compounds were evaluated against cancerous cervical cells in addition to evaluating the activity of the most active candidates against the target EGFR tyrosine kinase. Moreover, the cell cycle activity was detected for the most potent compound, to get an overview about the possible stage at which the new derivatives could suppress the growth of cancer cells. Also, up regulation ofp53, Bax/ Bcl-2ratio andcaspases -3 and -7 was also determined in this study.

2. Results and discussion

2.1. Chemistry

The target 2-(((3-(benzofuran-2-yl)-1-phenyl-1*H*-pyrazol-4-yl)methylene)hydrazono)-5-(aryl)thiazolidin-4-ones **(4–22)** were prepared in good yields using the following synthetic protocol. Firstly, the intermediate carbothioamide **2** [20] was allowed to react with ethyl bromoacetate in absolute ethanol containing few drops of piperidine as a catalytic basic medium to afford the corresponding 2-(((3-(benzofuran-2-yl)-1-phenyl-1*H*-pyrazol-yl)methylene)hydrazono)thiazolidin-4-one **(3)**. The new hybrids **4–22** were obtained via subjecting the key reactant thiazolidin-4-one **3** to Knoevenagel condensation reaction with a

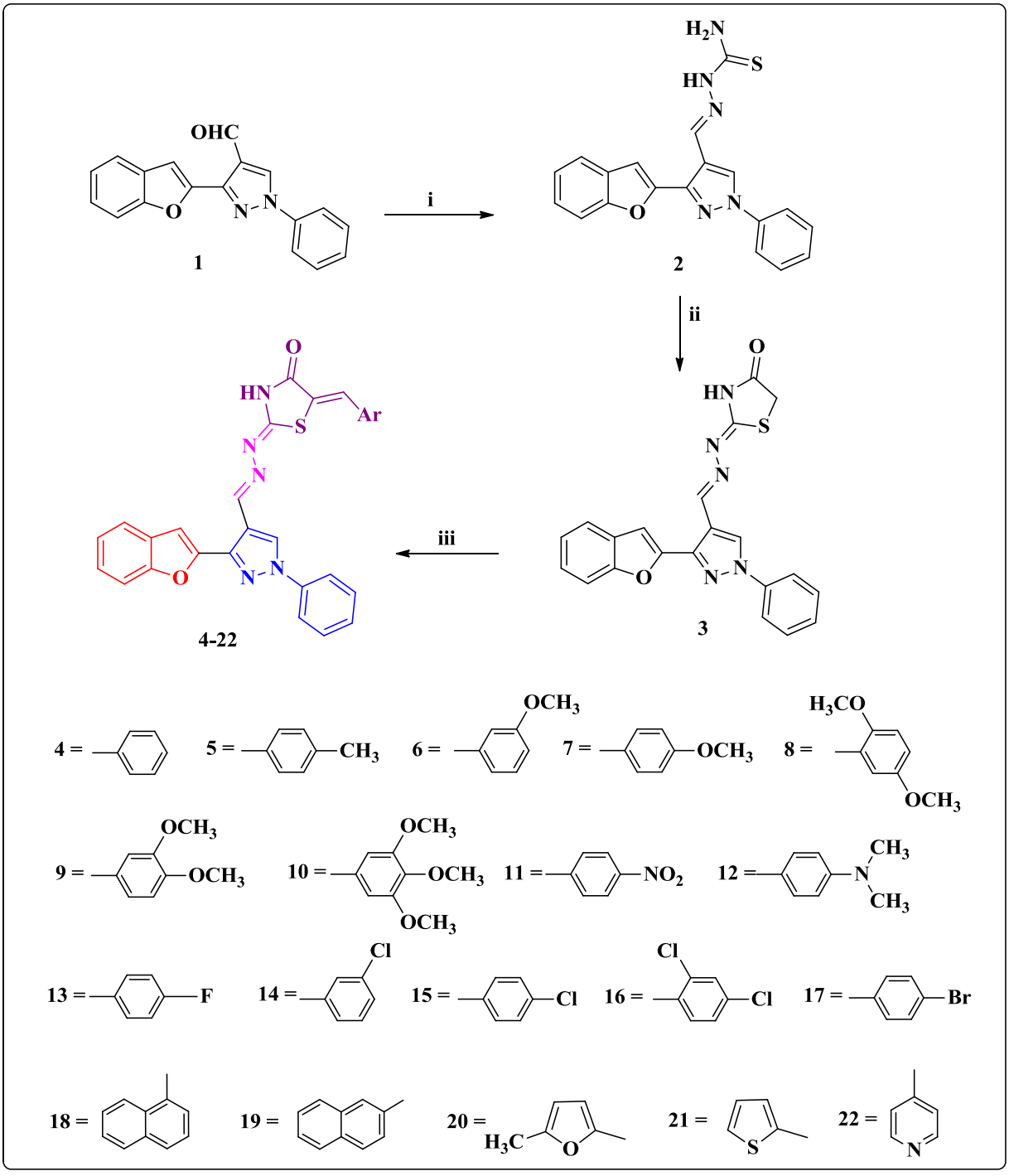

Scheme 1. Synthesis of new 2-(((3-(benzofuran-2-yl)-1-phenyl-1*H*-pyrazol-4-yl)methylene)hydrazono)-5-(aryl)thiazolidin-4-one derivatives. Reagents and conditions: (i) $NH_2CSNHNH_2$, EtOH, CH_3COOH, reflux 2 h; (ii) $BrCH_2COOEt$, EtOH, piperidine, reflux 3 h; (iii) different aromatic aldehydes, alcoholic NaOH (10%), stirring overnight.

series of aromatic and heterocyclic aldehydes in alcoholic sodium hydroxide with continuous stirring at room temperature overnight (Scheme 1). IR, ^{1}H NMR, ^{13}C NMR, Mass spectra and the elemental analyses were used to confirm the new molecules. ^{1}H NMR chemical shifts allowed the characterization of the protons of the new derivatives that were presented at their expected regions, such as a singlet signal appeared at δ 2.36, 3.03 ppm due to the three protons of CH_3 groups of compounds **5**, **12**, respectively. The signals of aromatic protons appeared as multiplet signals in their characteristic regions. While the methoxy protons OCH_3 of compounds **6–10** presented as singlets at the range δ 3.71–3.82 ppm. Also, ^{13}C NMR spectral data showed the typical signals for the aliphatic carbons in the expected regions, such as the signal for CH_3 carbon of compounds **5**, **12** which appeared at δ 21.46, 33.92 ppm, respectively and the signals due to OCH_3 carbons of compounds **6–10** which are presented at the region δ 55.63–56.56 ppm.

2.2. Biological evaluation

2.2.1. In vitro anticancer activity

The aim of the present investigation is to synthesize a new series of benzofuran–pyrazol-hydrazono-thiazolidin-4-ones **(4–22)** to be evaluated as anticancer candidates against the human cervix epithelioid

Table 1
In vitro anticancer activity against carcinoma Hela cell line, *in vitro* radiometric EGFR PK assay and the effects against the normal human cervix cells of the different target compounds.

Compounds	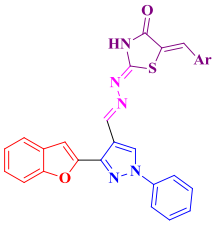 4–22 Ar	Anticancer activity against carcinoma Hela cell line IC_{50} (μM)	EGFR kinase inhibition. IC_{50} (μM)	The normal human cervical epithelium HCvEpC cell lines IC50 (μM)
3		4.80 ± 0.15		
4	C_6H_5	97.52 ± 3.19		
5	4-CH_3-C_6H_4	6.81 ± 0.22		
6	3-OCH_3-C_6H_4	0.63 ± 0.02	0.30	17.23
7	4-OCH_3-C_6H_4	0.82 ± 0.02	0.15	20.34
8	2,5-diOCH_3-C_6H_4	8.64 ± 0.28		
9	3,4-diOCH_3-C_6H_4	16.79 ± 0.55		
10	3,4,5-triOCH_3-C_6H_4	9.01 ± 0.29		
11	4-NO_2-C_6H_4	1.96 ± 0.06	0.40	17.67
12	4-$N(CH_3)_2$-C_6H_4	8.04 ± 0.26		
13	4-F-C_6H_4	2.52 ± 0.08	0.25	23.45
14	3-Cl-C_6H_4	2.99 ± 0.09	0.07	60.12
15	4-Cl-C_6H_4	22.68 ± 0.74		
16	2,4-diCl-C_6H_4	0.60 ± 0.01	0.22	20.34
17	4-Br-C_6H_4	1.03 ± 0.03	0.62	17.95
18	1-naphthlenyl	17.75 ± 0.58		
19	2-naphthlenyl	10.42 ± 0.34		
20	5-CH_3-furyl	4.90 ± 0.16		
21	2-thienyl	14.77 ± 0.48		
22	4-pyridyl	8.96 ± 0.29		
Doxorubicin		1.10 ± 0.15		
Erlotinib			0.08	

carcinoma cells. Accordingly, the anticancer activity of the new derivatives was assessed against Hella cell line using MTT assay [21–22]. Doxorubicin served as a standard drug. IC50 values for the tested compounds are reported in Table 1. It could be noted from the obtained data that the significance of the potency depends of the type of the substituents of the phenyl ring hybridized with the thiazolidinone ring. The most potent activity was gained by the 2,4-dichlorobenzylidene derivative **16** which was twice that obtained by the reference doxorubicin (IC50; 0.60 μM, $IC50_{Doxorubicin}$; 1.10 μM). Also, the 4-bromo derivative **17** produced equipotent activity to that of doxorubicin. The presence of the two chlorine or the bromine substituents on the phenyl ring yields an electron withdrawing effect. Even so, the halogen atoms increased the Lipophilicity of the molecules, which is considered as one reason for enhancement of the anticancer activity of the compounds **16**, **17**. On the other hand, the mono halo substitution of the phenyl ring as 4-fluoro/3-chloro derivatives **13**, **14** halved their activities when compared to the reference drug (IC50; 2.52, 2.99 μM, respectively). Dramatic reduction in the potency was observed by the 4-chloro derivative **15** (IC50; 22.68 μM). At the same time, the 3- and 4-methoxybenzylidene analogues **6**, **7** represented significant cytotoxic activity of about 1.8 or 1.3 folds higher than that of doxorubicin (IC50; 0.63, 0.82 μM, respectively), a result which could be explained due to the oxygen atom of the methoxy group that can function as H-bond acceptor with the target protein kinase. A reverse result was obtained upon increasing the number of the methoxy substituents on the phenyl ring. It was detected that 2,5-/3,4-/3,4,5-dimethoxybenzylidene analogues **8**, **9**, **10** and 4-(dimethylamino)benzylidene derivative **12** exhibited 8–16 folds reduction in the potency with respect to doxorubicin (IC50; 8.64, 16.79, 9.01, 8.04 μM, respectively). The increase in the bulkiness of the substituents might negatively affect the potency by changing the geometry of the molecules. Unfortunately, a detectable drop in the activity was observed by the unsubstituted phenyl derivative **4** (IC50; 97.52 μM). Furthermore, the replacement of the phenyl ring with two fused aromatic ring substituents such as 1-naphthalenyl and 2-naphthalenyl analogues **18**, **19** or with different heterocyclic rings such as; 5-CH_3-furyl, thienyl, pyridyl derivatives **20**, **21**, **22** was not in the favor the potency of the anticancer activity since the effect decreased by 4.45–16 folds regarding to doxorubicin

2.2.2. EGFR PK inhibition assay

EGFR PK inhibition activity was evaluated for the compounds that represented the most potent anticancer activity **6**, **7**, **11**, **13**, **14**, **16**, **17** using Hela cancer cells. The obtained results revealed that some of the tested compounds are promising EGFR PK inhibiting candidates (Table 1). Comparing to the potent EGFR PK inhibiting drug erlotinib, the 3-chlorobenzylidene compound **14** exhibited the most pronounced activity of IC50; 0.07 μM, more potent than the reference drug of IC50; 0.08 μM. Although the rest of the examined derivatives produced potent cytotoxic activity, their EGFR PK inhibitory activity was less than the reference drug by about 1.8–7.5 folds (IC50; 0.15–0.62 μM). In the light of the obtained results, although compound **14** represented the highest potency against EGFR PK, it showed the least anti-proliferative activity among the tested derivatives (2.99 ± 0.09 μM). Such discrepancies between enzyme potency and the anticancer activity are frequently problematic issues in the field of the development of new enzyme inhibiting agents. There are many factors that are related to such issue, such as improper physicochemical properties leading to less accumulation in the cancer cells [24,25]. In addition, there is no direct correlation between the anti-angiogenic effects of the tested compounds and their anticancer activity against Hela cells, since the *in vitro* conditions do not simulate the *in vivo* conditions since there is no blood supply or vascular endothelial cells [26]. So that, the cytotoxic effect of the synthesized compounds is not necessarily related to the EGFR PK inhibition, but mainly contribute to another mechanism of action.

2.2.3. Effect of various representative target compounds against thenormal cervical cells

Damage to the normal cells is a very important obstacle that occurs due to the great toxicity of antiproliferative drugs. Thus, the derivatives that showed the best activity against the cervix cancer (Hela) cells (**6**, **7**, **11**, **13**, **14**, **16**, **17**) were selected as representative compounds to be examined against the normal human cervical epithelium HCvEpC cell lines and their IC50 were determined via MTT assay [21–23]. It was detected that, the IC50 doses of all the tested analogues against the healthy cells were much higher than their IC50 doses against the affected cells (> 20 folds of IC50; 17.2–32.12 μM) (Table 1), confirming the safety profile of the tested compounds.

2.2.4. Cell cycle analysis and apoptosis assay

The most effective EGFR PK inhibiting candidate **14** was subjected to cell cycle analysis and apoptotic assay.

2.2.4.1. Cell cycle analysis and apoptosis detection. Typical neoplastic cells evade apoptosis since accumulation of mutations block apoptosis pathways. Numerous anticancer researches confirmed the induction of apoptosis upon effective cancer treatment. Autophagy is a metabolic process that degrades intracellular macromolecules and endogenous substrate to maintain a stable internal environment. It is an important regulatory mechanism in cell growth, maturation and death and is associated with a variety of human diseases, including tumors. Chemotherapy agents may lead to an autophagic response, which is one possible method of inducing apoptosis. There is a unique association between autophagy and apoptosis [27].While chemotherapeutic drugs induce autophagy, cell cycle arrest and cell senescence [21,22], it is imperative the induction of apoptosis and permanent removal of neoplastic cells for effective cancer treatment. Studies on the effect of compound **14** on cell cycle development and induction of apoptosis in cancer Hela cells was carried out. The cancer cells were incubated with the compound **14** at its IC50 concentration 2.99 μM for 24 h. The cells were stained with Annexin V/PI and analyzed by flow cytometry technique. Investigation of the resultant data (Fig. 3) revealed a high percentage of cell accumulation of 27.11% at pre G1 phase in Hela cells treated with the tested derivative after 24 h incubation *vs* 1.39% of the untreated Hela cells, indicating cell cycle arrest at G1/S phase.

2.2.4.2. Apoptosis assay. Cell cycle assay of Hela cancer cells treated with compound **14** showed the appearance of pre-G1 peak which emphasized the induction of apoptosis. To prove the potency of compound**14** to induce apoptosis, the cells were stained with Annexin V/PI, incubated for 24 h and analyzed. It has been detected that the early and late apoptosis produced by the examined compound **14** certainly indicated its capability to induce significant levels of apoptosis with necrosis percent 1.99 (Fig. 4). Also, the percentage of late apoptosis (16.57%) induced by compound **14** was higher than that of the early apoptosis (8.55%) which making recovery of apoptotic cells to be healthy is more difficult (Fig. 5).

2.2.4.3. Effect of compound 14 on the level of p53/Bax/ Bcl-2. Apoptosis is triggered in a cell via two main pathways, which are; the extrinsic pathway (the death receptor) or the intrinsic pathway (mitochondrial pathway) [28]. The cancer cells can resist apoptosis by modulating the expression of Bcl-2 family proteins which in turn regulate the mitochondrial apoptotic pathway via production anti-apoptotic proteins as Bcl-2 or down regulating pro-apoptotic proteins, such as Bax [29]. Accordingly, the expression of Bcl-2 and Bax genes is controlled by the tumor suppressor gene p53 [30]. Thus, this study also represented the impact of **14** on p53 expression and the ratio of Bax/ Bcl-2 (Table 2). Hela cells were exposed to compound **14** at its IC50 concentration 2.99 μM for 24 h. The tested compound **14** represented overexpression of the tumor suppressor gene p53 and the pro-apoptotic protein Bax by 7.07 and 5.7 folds, respectively with concurrent reduction in the expression levels ofthe anti-apoptotic protein Bcl-2 by 0.45 folds (Table 2). Consequently, an observable increase in Bax/Bcl-2 ratio was detected. These results suggested the participation of p53, Bax and Bcl-2 proteins in the apoptotic act of compound **14**.

2.2.4.4. Upregulation of caspases-3 and -7. Caspase cascade events mediate the induction of cell apoptosis via various intrinsic or extrinsic pathways. Activated caspase-3 and caspase-7 can cleave multiple structural and regulatory proteins, which are critical for cell survival and maintenance [31]. In this experiment, the bioluminescent intensities of caspases -3 and -7 indicated that their activities were measured in Hela cells treated with IC50 concentration of compound **14** for 24 h of treatment. As shown in (Table 3), a pronounced elevation in the caspases -3 and -7 levels by 16.21 and 7.60foldsrespectively comparing to the untreated Hela cells.

3. Molecular docking study

Molecular docking study was carried out to investigate the binding mode of interaction of the most potent EGFR PK inhibiting compound **14** to show its interactions with the key amino acids (hot spots) in the active site of the EGFR PK with the aim of explaining its promising inhibitory activity. All the molecular modeling studies were carried out

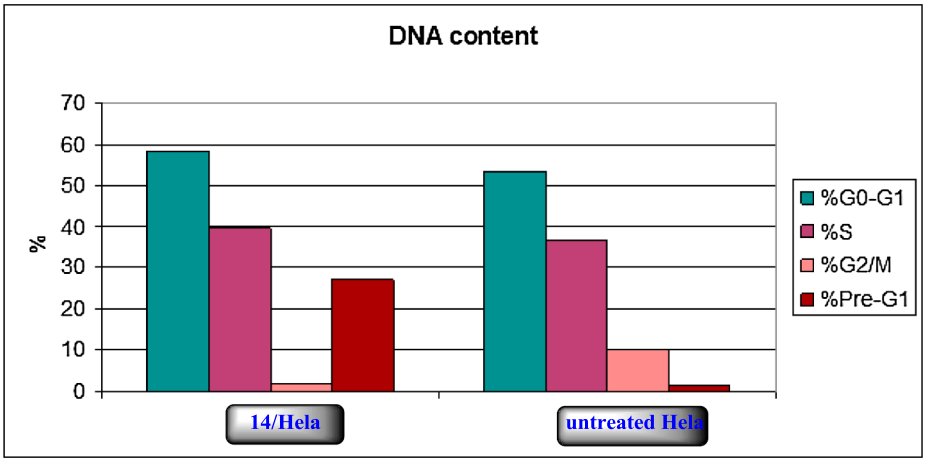

Fig. 3. Cell Cycle analysis results of compound **14**.

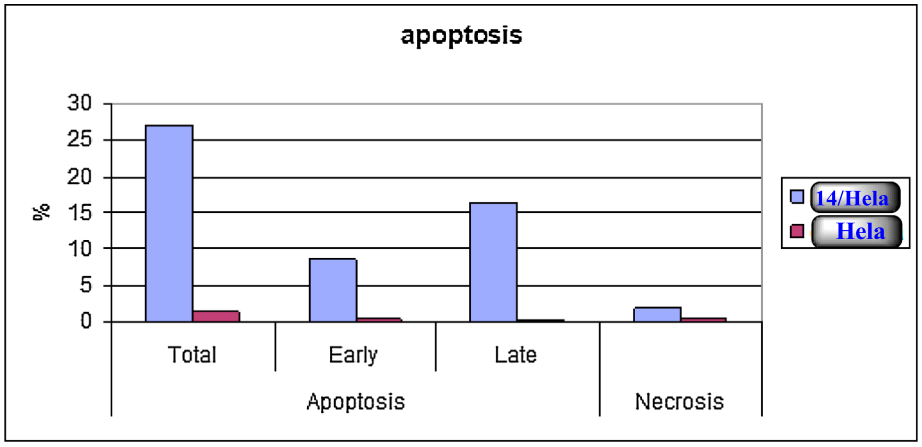

Fig. 4. Apoptosis induction analysis using Annexin V/PI for compound **14**.

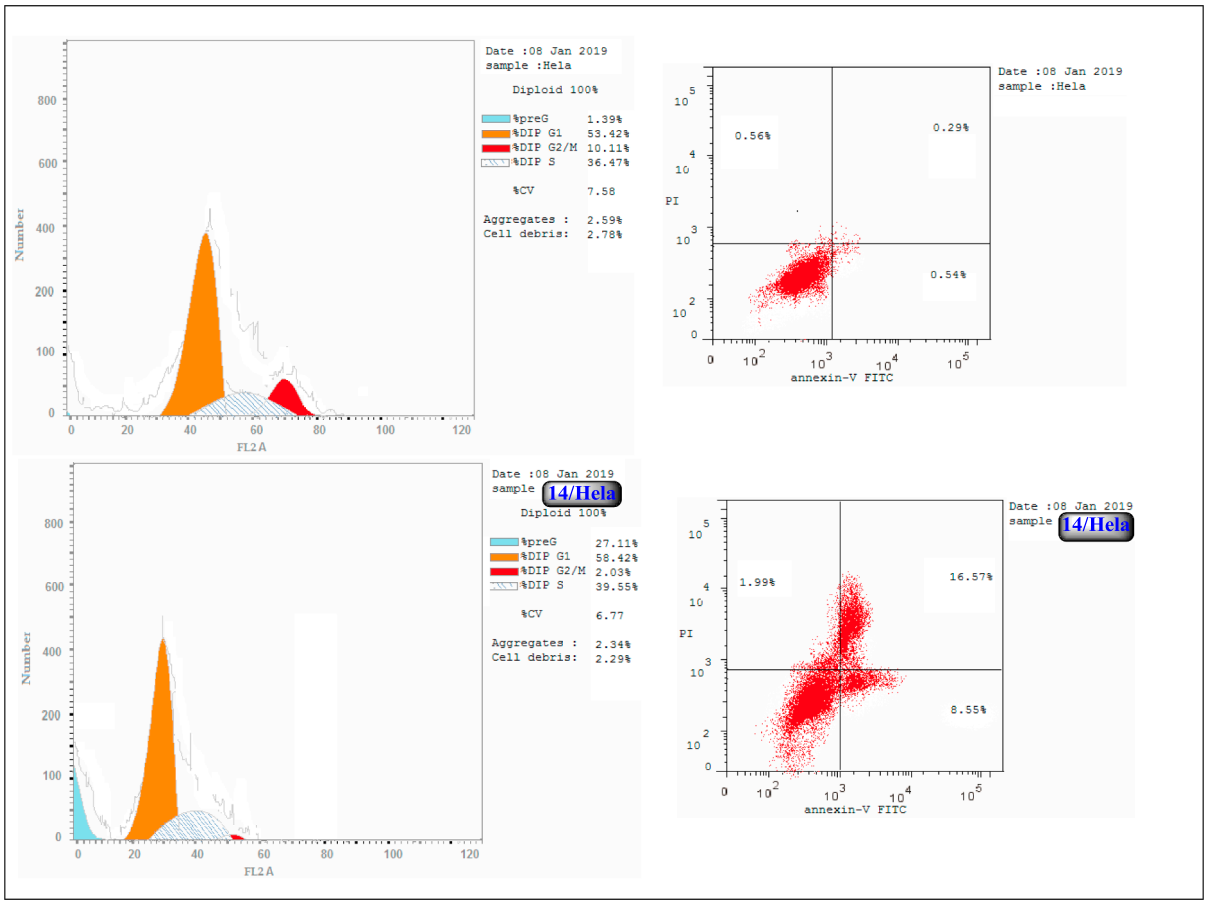

Fig. 5. Cell cycle analysis and apoptosis induction analysis of compound **14** on Hela cells.

Table 2
Results of p53/Bax/BCL-2 analysis after treatment of Hela cells with compound **14** for 24 h.

Compound	Conc. (μM)	Conc. Pg/mL Bax	Bax fld	Conc. ng/mL Bcl-2	Bcl-2 fld	Conc. Pg/mL p53	p53 fld
14	2.99 μM	232.2 ± 9.5	5.7	2.58 ± 0.18	0.45	654.5 ± 22.8	7.07
Control	–	40.63 ± 2.9	1	5.7 ± 0.31	1	92.54 ± 3.89	1

using Molecular Operating Environment (MOE, 2010.10) software. All minimizations were performed with MOE until an RMSD gradient of 0.05 kcal mol^{-1} $Å^{-1}$ with MMFF94x force field and the partial charges were automatically calculated [32,33]. H-bonding with Met769, through water mediated H-bonding with Thr766 and cation-π interaction with Lys721 (Figs. 6 and 7). The validated setup was then used in predicting the ligand-receptor interactions at the binding site for the compound of interest.

Table 3
Caspases-3, -7 concentrations in Hela cells after treatment with compound **14** for 24 h.

Cell line	Conc. pg/mL Casp-3	Folds	Conc. ng/mL Casp-7	Folds
Hela cells treated with compound **14**	274.6	16.21	1.516	7.60
Untreated Hela cells (control)	16.93	1	0.1994	1

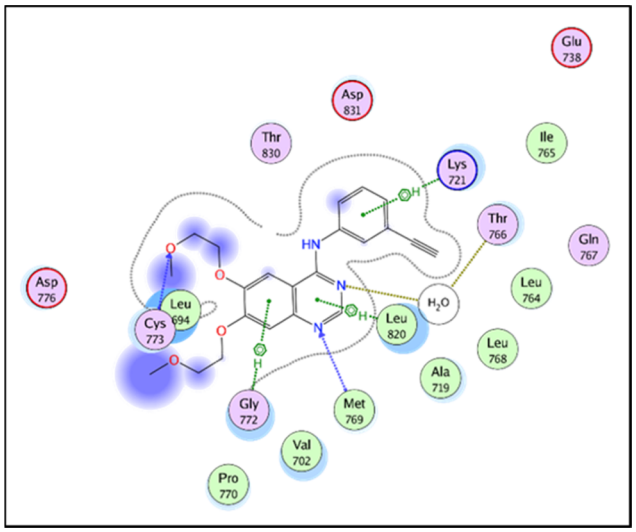

Fig. 6. 2D interaction diagram showing erlotinib docking pose interactions with the key amino acids in the EGFR PK binding site.

The ability of compound **14** to interact with the key amino acids in the binding site rationalizes its good activity as indicated by its docking pattern and docking score compared to that of erlotinib. The general binding pattern of the tested compound **14** is that it interacts through hydrogen bonding with the key amino acid Met769 by its N atom of the imine moiety, through water mediated H-bonding with Thr766 by its S atom of the thiazole ring and through cation-π interaction with Lys721 by its *m*-chlorophenyl moiety **(**Fig. 8 and Table 4**)**.

4. Conclusion

A new series of 2-(((3-(benzofuran-2-yl)-1-phenyl-1*H*-pyrazol-4-yl) methylene)hydrazono)-5-(aryl)thiazolidin-4-one derivatives have been designed and synthesized as anticancer EGFR kinase inhibitors. All the new derivatives were subjected to anticancer evaluation against Hela cell line by MTT technique using doxorubicin as a standard drug. The compounds **6**, **7**, **11**, **13**, **14**, **16**, **17** exhibited the most potent activity of IC50 values ranging from 0.60 to 2.99 μM comparing to 1.10 μM the IC50 value of doxorubicin. Furthermore, the latter derivatives were evaluated for their EGFR kinase inhibitory activity. The 3-chlorobenzylidene compound **14** represented the highest inhibitory activity among all the tested compounds more than the reference drug erlotinib of IC50; 0.07 μM *vs* $IC50_{erlotinib}$; 0.08 μM. Also, compound **14** showed high cell accumulation at pre G1 phase in Hela cells confirming its arresting cellcycle at G1/S phase. Compound **14** was certainly able to induce significant levels of apoptosis percent 27.11%. The apoptotic mechanistic pathway of **14** was also emphasized by the enhanced expression of the tumor suppressor gene p53 and the increase of Bax/Bcl-2 ratio. In addition, a pronounced enhancement in the levels of the active caspases -3 and -7 was also investigated indicating the potent pro apoptotic activity of **14** by inducing the intrinsic apoptotic pathway. Molecular docking study of compound **14** represented its good fitting and proper interaction with the key amino residues in the binding site of EGFR kinase comparing to erlotinib.

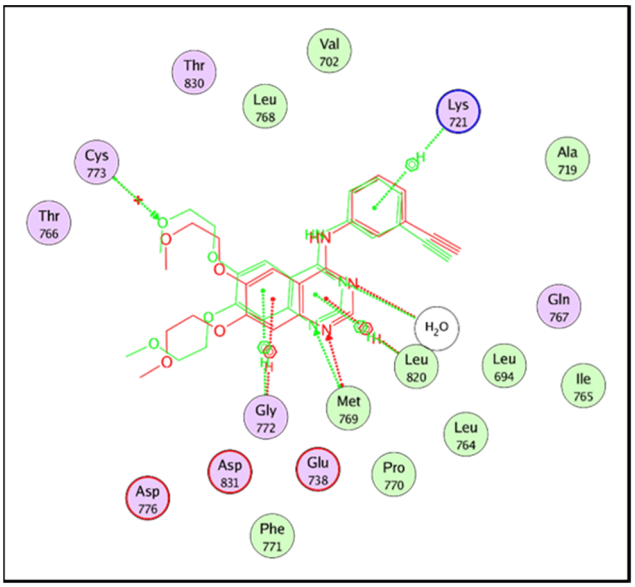

(a)

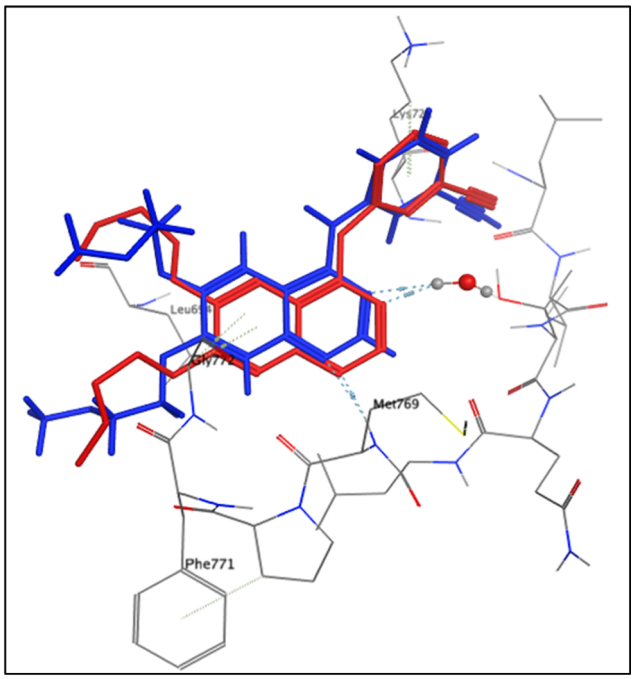

(b)

Fig. 7. (a) 2D representation and (b) 3D representation of the superimposition of the co-crystallized (red) and the docking pose (blue) of erlotinib in the EGFR PK binding site with RMSD of 1.321 Å. (Ligand Hydrogen atoms were removed for clarity).

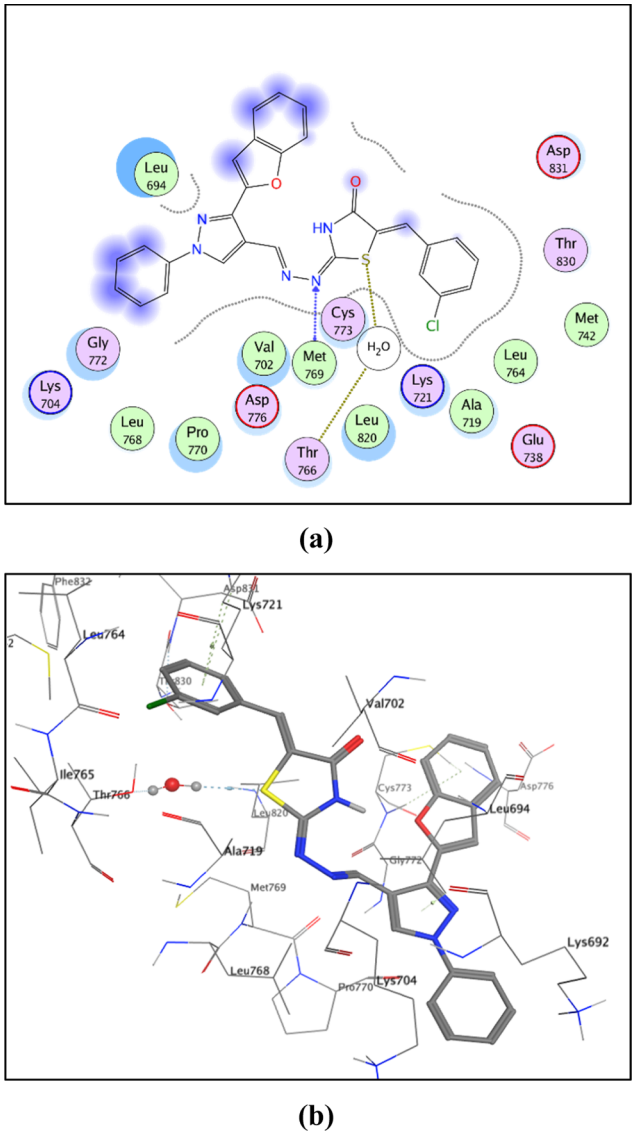

Fig. 8. (a) 2D diagram and (b) 3D representation of compound **14** in the EGFR PK binding site.

Table 4
Docking energy scores (*S*) in kcal/mol for the reference drug and the tested compound **14.**

Compound	Docking score (kcal/mol)
Erlotinib	−11.07
14	−11.49

5. Experimental

5.1. Chemistry

All melting points are uncorrected and were taken in open capillary tubes using Electrothermal apparatus 9100. Elemental microanalyses were carried out at Microanalytical Unit, Central Services Laboratory, National Research Centre, Dokki, Cairo, Egypt, using Vario Elementar and were found within ± 0.4% of the theoretical values. Infrared spectra were recorded on a Schimadzu FT-IR Affinity-1 Spectrometer, Infrared spectrometer at cm^{-1} scale using KBr disc technique at Faculty of Pharmacy-Cairo University, Cairo, Egypt. ^{1}H NMR and ^{13}C NMR spectra were determined by using a Bruker High Performance Digital FT-NMR Spectrometer Avance III 400 MHz, Faculty of Pharmacy-Cairo University, Cairo, Egypt. Chemical shifts were expressed in δ (ppm) downfield from TMS as an internal standard. The mass spectrawere measured with a Finnigan MATSSQ-7000 mass spectrometer at Central Services Laboratory, National Research Centre, Dokki, Cairo, Egypt. Follow up of the reactions and checking the purity of the compounds were made by TLC on silica gel-precoated aluminum sheets (Type 60, F 254, Merck, Darmstadt, Germany) using chloroform/methanol (20:2, v/v) and the spots were detected by exposure to UV lamp at λ254 nm for few seconds and by iodine vapor. The chemical names given for the prepared compounds are according to the IUPAC system. 3-(Benzofuran-2-yl)-1-phenyl-1*H*-pyrazole-4-carbaldehyde (**1**), 2-((3-(benzofuran-2-yl)-1-phenyl-1*H*-pyrazol-4-yl)methylene)hydrazine-1-carbothioamide (**2**) were prepared according to the reported method [17].

*5.1.1. 2-(((3-(Benzofuran-2-yl)-1-phenyl-1H-pyrazol-4-yl)methylene) hydrazono)thiazolidin-4-one (**3**)*

A mixture of 2-((3-(benzofuran-2-yl)-1-phenyl-1*H*-pyrazol-4-yl)methylene)hydrazine-1-carbothioamide (**2**) (7.22 g, 0.02 mol) and ethyl bromoacetate (3.52 mL, 0.02 mol) was dissolved in absolute ethanol (50 mL) containing a few drops of piperidine was refluxed for 3 h. The formed precipitate was filtered, dried and recrystallized from absolute ethanol to give the title compound **3**.

Yield 82%, mp 262–263 °C, light orange solid, IR (ν_{max}/cm^{-1}): 3135 (NH), 3051 (CH-aromatic), 1711 (C=O), 1631 (C=N), 1598 (C=C). ^{1}H NMR (DMSO-d_6): δ 3.98 (s, 2H, thiazolidinone protons), 7.30–7.33 (m, 1H, Ar-H), 7.37–7.45 (m, 2H, Ar-H), 7.57–7.60 (s, 2H, Ar-H), 7.70–7.75 (s, 2H, Ar-H), 7.88 (s, 1H, Ar-H), 8.00 (d, 2H, Ar-H, J = 7.92 Hz), 8.73 (s, 1H, CH=N proton), 9.04 (s, 1H, pyrazole proton), 11.02 (br s, 1H, NH, D_2O exchangeable);^{13}C NMR (DMSO-d_6): δ 55.68 (CH_2), 107.39, 111.83, 114.73, 119.34, 121.79, 122.35, 123.76, 125.69, 127.73, 128.78, 130.18, 131.06, 132.31, 139.24, 141.72, 143.98, 149.84, 154.67, 159.36, 174.18 (C=O). MS, m/z(%): 401 [M^+] (33), 77 [C_6H_5] (100). Anal. For $C_{21}H_{15}N_5O_2S$ (401.44): Calcd. C, 62.83; H, 3.77; N, 17.45; S, 7.99; Found: C, 62.56; H, 3.44; N, 17.27; S, 7.61.

5.1.2. General procedure for the synthesis of 2-(((3-(benzofuran-2-yl)-1-phenyl-1H-pyrazol-4-yl)methylene)hydrazono)-5-(aryl)thiazolidin-4-one 4–22

A mixture of thiazolidin-4-one derivative **3** (0.41 gm, 0.001 mol) and the appropriate aldehyde namely; benzaldehyde, 4-methylbenzaldehyde, 3-methoxybenzaldehyde, 4-methoxybenzaldehyde, 2,5-dimethoxybenzaldehyde, 3,4-dimethoxybenzaldehyde, 3,4,5-trimethoxybenzaldehyde, 4-nitrobenzaldehyde, 4-(dimethylamino)benzaldehyde, 4-fluorobenzaldehyde, 3-chlorobenzaldehyde, 4-chlorobenzaldehyde, 2,4-dichlorobenzaldehyde, 4-bromobenzaldehyde, 1-naphthaldehyde, 2-naphthaldehyde, 5-methylfuran-2-carbaldehyde, thiophene-2-carbaldehyde and pyridine-4-carbaldehyde (0.0015 mol) was dissolved in alcoholic sodium hydroxide (20 mL, 10%) was continuously stirred at room temperature overnight. The formed precipitate was filtered, washed several times with water, dried and crystallized from acetic acid to afford the title compounds **4–22** respectively.

*5.1.2.1. 2-(((3-(Benzofuran-2-yl)-1-phenyl-1H-pyrazol-4-yl)methylene) hydrazono)-5-(benzylidene)thiazolidin-4-one (**4**).* Yield 88%, mp 284–285 °C, yellow solid, IR (ν_{max}/cm^{-1}): 3132 (NH), 3059 (CH-aromatic), 1709 (C=O), 1637 (C=N), 1597 (C=C). ^{1}H NMR (DMSO-d_6): δ 7.26–7.75 (m, 11*H*, Ar-H), 7.84 (s, 1H, CH=C), 7.97–8.05 (m, 4H, Ar-H), 8.84 (s, 1H, CH=N proton), 9.17 (s, 1H, pyrazole proton), 12.68 (br s, 1H, NH, D_2O exchangeable); ^{13}C NMR (DMSO-d_6): δ 107.30, 107.94, 111.72, 111.90, 117.46, 119.50, 119.64, 121.91, 123.71, 123.95, 125.75, 125.84, 126.18, 127.93, 128.08, 128.49, 128.55, 128.76, 129.69, 130.19, 130.31, 131.30, 131.75, 134.10, 139.14, 149.42, 154.77, 174.01. MS, *m/z* (%): 489 [M^+] (22), 77 [C_6H_4] (100). Anal. For $C_{28}H_{19}N_5O_2S$ (489.55): Calcd. C,

68.70; H, 3.91; N, 14.31; S, 6.55; Found: C, 68.56; H, 3.78; N, 14.47; S, 6.30.

*5.1.2.2. 2-(((3-(Benzofuran-2-yl)-1-phenyl-1H-pyrazol-4-yl)methylene) hydrazono)-5-(4-methylbenzylidene)thiazolidin-4-one (**5**)*. Yield 78%, mp 223–225 °C, dark yellow solid, IR (ν_{max}/cm^{-1}): 3129 (NH), 3047 (CH-aromatic),1704 (C═O), 1632 (C═N), 1597 (C═C).^{1}H NMR (DMSO-d_6): δ 2.36 (s, 3H, CH_3), 7.26–7.42 (m, 6H, Ar-H), 7.55–7.61 (m, 4H, Ar-H), 7.75–7.76 (m, 2H, Ar-H), 8.03 (d, 2H, Ar-H, J = 7.22 Hz), 8.09 (s, 1H, CH═C), 8.73 (s, 1H, CH═N proton), 9.03 (s, 1H, pyrazole proton), 12.03 (br s, 1H, NH, D_2O exchangeable);^{13}C NMR (DMSO-d_6): δ21.46 (CH_3), 107.39, 111.83, 119.14, 119.38, 121.80. 122.49, 123.77, 125.64, 127.68, 128.82, 129.50, 129.88, 130.16, 131.84, 133.73, 137.89, 139.32, 141.75, 144.28, 149.93, 154.70, 179.64 (C═O). MS, *m/z* (%): 503 [M$^+$] (29), 91 [C_7H_7] (100). Anal. For$C_{29}H_{21}N_5O_2S$ (503.58): Calcd. C, 69.17; H, 4.20; N, 13.91; S, 6.37; Found: C, 69.28; H, 4.35; N, 13.72; S, 6.18.

*5.1.2.3. 2-(((3-(Benzofuran-2-yl)-1-phenyl-1H-pyrazol-4-yl)methylene) hydrazono)-5-(3-methoxybenzylidene)thiazolidin-4-one (**6**)*. Yield 77%, mp 259–260 °C, canarysolid,IR (ν_{max}/cm^{-1}): 3125 (NH), 3048 (CH-aromatic), 2947, 2836 (CH-aliphatic), 1716 (C═O), 1639 (C═N), 1597 (C═C).^{1}H NMR (DMSO-d_6): δ 3.72 (s, 3H, OCH_3), 6.99 (d, 1H, Ar-H, J = 8.92 Hz), 7.19–7.17 (m, 2H, Ar-H), 7.25–7.39 (m, 4H, Ar-H), 7.50–7.55 (m, 3H, Ar-H), 7.65 (d, 2H, Ar-H, J = 8.00 Hz), 7.81 (s, 1H, CH═C), 7.96 (d, 2H, Ar-H, J = 8.04 Hz), 8.74 (s, 1H, CH═N proton), 9.07 (s, 1H, pyrazole proton), 12.57 (br s, 1H, NH,D_2O exchangeable); ^{13}C NMR (DMSO-d_6): δ55.63 (OCH_3), 107.52, 111.76, 115.29, 115.87, 117.84, 119.52, 121.75, 121.92, 123.89, 124.02, 125.86, 128.03, 128.52, 130.23, 130.64, 131.30, 139.08, 149.42, 154.66, 160.03, 174.28 (C═O).MS, *m/z* (%): 518 [M^{-1}] (18), 76 [C_6H_4] (100). Anal. For$C_{29}H_{21}N_5O_3S$ (519.58): Calcd. C, 67.04; H, 4.07; N, 13.48; S, 6.17; Found: C, 67.26; H, 4.30; N, 13.25; S, 6.02.

*5.1.2.4. 2-(((3-(Benzofuran-2-yl)-1-phenyl-1H-pyrazol-4-yl)methylene) hydrazono)-5-(4-methoxybenzylidene)thiazolidin-4-one (**7**)*. Yield 84%, mp 297–298 °C, yellow solid,IR (ν_{max}/cm^{-1}): 3138 (NH), 3058 (CH-aromatic),1710 (C═O), 1629 (C═N), 1594 (C═C).^{1}H NMR (DMSO-d_6): δ 3.82 (s, 3H, OCH_3), 7.00 (d, 2H, Ar-H, J = 8.56 Hz), 7.22 (s, 1H, Ar-H), 7.35–7.44 (m, 3H, Ar-H), 7.57–7.62 (m, 4H, Ar-H), 7.74–7.77 (m, 2H, Ar-H), 8.03 (d, 2H, Ar-H, J = 7.92 Hz), 8.10 (s, 1H, CH═C), 8.69 (s, 1H, CH═N proton), 9.00 (s, 1H, pyrazole proton), 12.31 (br s, 1H, NH, D_2O exchangeable);^{13}C NMR (DMSO-d_6): δ 56.56 (OCH_3), 107.37, 111.69, 114.81, 117.65, 119.48, 122.04, 123.83, 125.75, 127.96, 128.05, 128.35, 128.51, 130.15, 130.83, 133.38, 139.06, 142.28, 143.61, 144.41, 149.38, 149.61, 154.66, 164.49, 165.31, 174.69 (C═O). MS, *m/z* (%): 519 [M$^+$] (25), 77 [C_6H_5] (100). Anal. For$C_{29}H_{21}N_5O_3S$ (519.58): Calcd. C, 67.04; H, 4.07; N, 13.48; S, 6.17; Found: C, 67.32; H, 4.29; N, 13.19; S, 6.41.

*5.1.2.5. 2-(((3-(Benzofuran-2-yl)-1-phenyl-1H-pyrazol-4-yl)methylene) hydrazono)-5-(2,5-dimethoxybenzylidene)thiazolidin-4-one (**8**)*. Yield 76%, mp 283-285°Ccanarysolid,IR (ν_{max}/cm^{-1}): 3136 (NH), 3043 (CH-aromatic), 2939, 2831 (CH-aliphatic), 1712 (C═O), 1632 (C═N), 1597 (C═C). ^{1}H NMR (DMSO-d_6): δ 3.71 (s, 3H, OCH_3), 3.83 (s, 3H, OCH_3),7.08–7.10 (m, 3H, Ar-H), 7.27–7.46 (m, 3H, Ar-H), 7.57–7.61 (m, 2H, Ar-H), 7.67–7.72 (m, 2H, CH═C, Ar-H), 7.84 (d, 2H, Ar-H, J = 10.67 Hz), 8.03 (d, 2H, Ar-H, J = 7.88 Hz), 8.82 (s, 1H, CH═N proton), 9.14 (s, 1H, pyrazole proton), 12.60 (br s, 1H, NH,D_2O exchangeable); ^{13}C NMR (DMSO-d_6): δ 55.89 (OCH_3), 56.05 (OCH_3), 107.54, 111.61, 112.24, 114.05, 115.28, 118.08, 119.18, 119.32, 121.91, 122.54, 122.94, 123.82, 125.61, 127.68, 128.43, 130.22, 133.31, 139.25, 142.19, 143.27, 147.86, 149.01, 149.62, 150.11, 154.58, 173.43 (C═O). MS, *m/z* (%): 548 [M^{-1}] (21), 91 [C_7H_7] (100).Anal. For$C_{30}H_{23}N_5O_4S$ (549.61): Calcd. C, 65.56; H, 4.22; N, 12.74; S, 5.83; Found: C, 65.40; H, 4.36; N, 12.58; S, 5.65.

*5.1.2.6. 2-(((3-(Benzofuran-2-yl)-1-phenyl-1H-pyrazol-4-yl)methylene) hydrazono)-5-(3,4-dimethoxybenzylidene)thiazolidin-4-one (**9**)*. Yield 78%, mp 249–250 °C, light yellow,IR (ν_{max}/cm^{-1}): 3124 (NH), 3059 (CH-aromatic), 2951, 2831 (CH-aliphatic), 1701 (C═O), 1635 (C═N), 1593 (C═C).^{1}H NMR (DMSO-d_6): δ 3.76 (s, 3H, OCH_3), 3.83 (s, 3H, OCH_3), 7.04 (d, 1H, Ar-H, J = 8.16 Hz), 7.23–7.25 (m, 2H, Ar-H), 7.31–7.35 (m, 1H, Ar-H), 7.39–7.45 (m, 2H, Ar-H), 7.51 (s, 1H, Ar-H), 7.58–7.61 (m, 2H, Ar-H), 7.71–7.75 (m, 2H, Ar-H), 7.89 (s, 1H, s, 1H, CH═C), 8.01 (d, 2H, Ar-H, J = 7.92 Hz), 8.78 (s, 1H, CH═N proton), 9.09 (s, 1H, pyrazole proton), 12.46 (br s, 1H, NH, D_2O exchangeable);^{13}C NMR (DMSO-d_6): δ 55.87 (OCH_3), 55.97 (OCH_3), 107.33, 111.76, 112.13, 114.23, 115.22, 118.14, 119.39, 119.45, 121.83, 122.41, 123.75, 125.72, 127.87, 128.59, 130.13, 133.11, 139.10, 142.11, 143.39, 147.98, 149.22, 149.55, 150.06, 154.65, 172.83 (C═O).MS, *m/z* (%): 550 [M^{+1}] (29), 77 [C_6H_5] (100). Anal. For$C_{30}H_{23}N_5O_4S$ (549.61): Calcd. C, 65.56; H, 4.22; N, 12.74; S, 5.83; Found: C, 65.72; H, 4.38; N, 12.50; S, 5.54.

*5.1.2.7. 2-(((3-(Benzofuran-2-yl)-1-phenyl-1H-pyrazol-4-yl)methylene) hydrazono)-5-(3,4,5-trimethoxybenzylidene)thiazolidin-4-one (**10**)*. Yield 71%, mp 206–207 °C,canarysolid,IR (ν_{max}/cm^{-1}): 3163 (NH), 3048 (CH-aromatic), 2936, 2835 (CH-aliphatic), 1701 (C═O), 1631 (C═N), 1585 (C═C).^{1}H NMR (DMSO-d_6): δ 3.71 (s, 3H, OCH_3), 3.72 (s, 6H, OCH_3), 6.95 (s, 2H, Ar-H), 7.20 (s, 1H, Ar-H), 7.24–7.45 (m, 2H, Ar-H), 7.58–7.75 (m, 3H, Ar-H), 7.92–8.01 (m, 2H, Ar-H), 8.32 (s, 1H, CH═C), 8.64 (d, 2H, Ar-H, J = 7.28 Hz), 8.84 (s, 1H, CH═N proton), 9.27 (s, 1H, pyrazole proton), 11.50 (s, 1H, NH, D_2O exchangeable); ^{13}C NMR (DMSO-d_6): δ 56.18 (2-OCH_3), 60.64 (OCH_3), 106.89, 107.03, 111.67, 118.45, 119.25, 119.40, 121.77, 122.05, 124.05, 125.68, 127.99, 128.05, 128.43, 128.64, 130.22, 130.25, 132.41, 135.45, 137.74, 139.21, 139.28, 141.74, 142.57, 149.52, 149.79, 153.41, 154.61, 178.11 (C═O).MS, *m/z* (%): 579 [M$^+$] (17), 90 [C_7H_6] (100). Anal. For $C_{31}H_{25}N_5O_5S$ (579.63): Calcd. C, 64.24; H, 4.35; N, 12.08; S, 5.53; Found: C, 64.06; H, 4.18; N, 12.24; S, 5.21.

*5.1.2.8. 2-(((3-(Benzofuran-2-yl)-1-phenyl-1H-pyrazol-4-yl)methylene) hydrazono)-5-(4-nitrobenzylidene)thiazolidin-4-one (**11**)*. Yield 60%, mp 286–287 °C, dark red solid,IR (ν_{max}/cm^{-1}): 3132 (NH), 3062 (CH-aromatic), 1713 (C═O), 1635 (C═N), 1597 (C═C).^{1}H NMR (DMSO-d_6): δ 7.32–7.44 (m, 4H, Ar-H), 7.58–7.74 (m, 6H, Ar-H), 7.96 (s, 1H, CH═C), 7.87 (d, 1H, Ar-H, J = 8.60 Hz), 8.03 (d, 2H, Ar-H, J = 7.60 Hz), 8.30 (d, 1H, Ar-H, J = 8.68 Hz), 8.81 (s, 1H, CH═N proton), 9.09 (s, 1H, pyrazole proton), 12.13 (br s, 1H, NH, D_2O exchangeable); ^{13}C NMR (DMSO-d_6): δ 107.15, 112.56, 117.92, 119.37, 120.38, 121.69, 122.23, 124.24, 125.74, 127.68, 128.21, 128.56, 129.07, 130.30, 132.51, 137.74, 138.43, 139.39, 141.62, 142.71, 149.77, 149.91, 152.81, 155.40, 177.66 (C═O). MS, *m/z* (%): 534 [M$^+$] (18), 77 [C_6H_5] (100). Anal. For$C_{28}H_{18}N_6O_4S$ (534.55): Calcd. C, 62.91; H, 3.39; N, 15.72; S, 6.00; Found: C, 62.75; H, 3.51; N, 15.62; S, 6.18.

*5.1.2.9. 2-(((3-(Benzofuran-2-yl)-1-phenyl-1H-pyrazol-4-yl)methylene) hydrazono)-5-(4-(dimethylamino)benzylidene)thiazolidin-4-one (**12**)*. Yield 61%, mp 259–260 °C, light orange solid,IR (ν_{max}/cm^{-1}): 3117 (NH), 3048 (CH-aromatic), 1732 (C═O), 1636 (C═N), 1582 (C═C).^{1}H NMR (DMSO-d_6): δ 3.03 (s, 6H, N(CH_3)$_2$), 6.78 (d, 1H, Ar-H, J = 8.72 Hz), 7.30–7.45 (m, 4H, Ar-H), 7.48–7.52 (m, 1H, Ar-H),7.57–7.61 (m, 3H, Ar-H), 7.70–7.75 (m, 3H, Ar-H), 7.89 (s, 1H, CH═C), 8.00 (d, 2H, Ar-H, J = 8.00 Hz), 8.73 (s, 1H, CH═N proton), 9.04 (s, 1H, pyrazole proton), 11.94 (br s, 1H, NH, D_2O exchangeable); ^{13}C NMR (DMSO-d_6): δ 33.92 (N(CH_3)$_2$), 107.34, 107.48, 111.78, 112.42, 117.78, 119.55, 121.89, 122.05, 123.86, 125.75, 127.96, 128.58, 130.18, 130.89, 132.12, 139.17, 142.31, 149.33, 149.48, 149.56, 151.31, 154.71, 154.76, 174.96 (C═O). MS, *m/z* (%): 533 [M^{+1}] (23), 77 [C_6H_5] (100). Anal. For $C_{30}H_{24}N_6O_2S$ (532.62): Calcd. C, 67.65; H, 4.54; N, 15.78; S, 6.02; Found: C, 67.49; H, 4.27; N, 15.60; S, 6.15.

5.1.2.10. 2-(((3-(Benzofuran-2-yl)-1-phenyl-1H-pyrazol-4-yl)methylene) hydrazono)-5-(4-fluorobenzylidene)thiazolidin-4-one ***(13)***. Yield 84%, mp 284–286 °C, yellow solid,IR (ν_{max}/cm^{-1}): 3132 (NH), 3063 (CH-aromatic),1715 (C═O), 1620 (C═N), 1589 (C═C).^{1}H NMR (DMSO-d_6): δ 7.23–7.28 (m, 2H, Ar-H), 7.33–7.44 (m, 4H, Ar-H), 7.57–7.61 (m, 2H, Ar-H), 7.67–7.77(m, 4H, Ar-H), 7.99 (s, 1H,CH═C),8.03 (d, 2H, Ar-H, J = 7.84 Hz),8.69 (s, 1H, CH═N proton), 8.99 (s, 1H, pyrazole proton), 11.87 (br s, 1H, NH, D_2O exchangeable); ^{13}C NMR (DMSO-d_6): δ 107.34, 112.04, 116.21, 117.64, 118.71, 119.58, 121.47, 122.11, 123.51, 123.90, 125.63, 128.70, 129.08, 129.71, 130.02, 130.75, 132.54, 140.48, 142.87, 149.28, 149.72, 151.46, 153.95, 156.62, 174.96 (C═O).MS, *m/z* (%): 506 [M^{-1}] (16), 77 [C_6H_5] (100). Anal. For$C_{28}H_{18}FN_5O_2S$ (507.54): Calcd. C, 66.26; H, 3.57; N, 13.80; S, 6.32; Found: C, 66.42; H, 3.29; N, 13.92; S, 6.16.

5.1.2.11. 2-(((3-(Benzofuran-2-yl)-1-phenyl-1H-pyrazol-4-yl)methylene) hydrazono)-5-(3-chlorobenzylidene)thiazolidin-4-one ***(14)***. Yield 72%, mp 243–245 °C, yellow solid,IR (ν_{max}/cm^{-1}): 3125 (NH), 3059 (CH-aromatic), 1713 (C═O), 1639 (C═N), 1597 (C═C).^{1}H NMR (DMSO-d_6): δ 7.30–7.45 (m, 3H, Ar-H), 7.52–7.61 (m, 5H, Ar-H), 7.70–7.75 (m, 3H, Ar-H), 7.80 (s, 1H,CH═C),7.88–7.96(m, 1H, Ar-H),8.01 (d, 2H, Ar-H, J = 8.16 Hz),8.82 (s, 1H, CH═N proton), 9.14 (s, 1H, pyrazole proton), 12.64 (br s, 1H, NH, D_2O exchangeable);^{13}C NMR (DMSO-d_6): δ 106.84, 111.36, 117.69, 119.90, 120.43, 121.56, 122.51, 123.22, 123.85, 124.80, 125.21, 125.68, 128.25, 128.96, 129.11, 129.62, 129.97, 131.06, 134.62, 139.04, 142.87, 148.20, 149.01, 151.13, 154.55, 174.82 (C═O). MS, *m/z* (%): 525, 523 [M$^+$] (23, 8), 77 [C_6H_5] (100). Anal. For$C_{28}H_{18}ClN_5O_2S$ (524.00): Calcd. C, 64.18; H, 3.46; N, 13.37; S, 6.12; Found: C, 64.27; H, 3.51; N, 13.14; S, 6.30.

5.1.2.12. 2-(((3-(Benzofuran-2-yl)-1-phenyl-1H-pyrazol-4-yl)methylene) hydrazono)-5-(4-chlorobenzylidene)thiazolidin-4-one ***(15)***. Yield 82%, mp > 300 °C, yellow solid,IR (ν_{max}/cm^{-1}): 3124 (NH), 3048 (CH-aromatic),1713 (C═O), 1636 (C═N), 1597 (C═C).^{1}H NMR (DMSO-d_6): δ 7.29–7.33 (m, 1H, Ar-H), 7.38–7.45 (m, 3H, Ar-H), 7.52–7.65 (m, 5H, Ar-H), 7.68–7.72 (m, 2H, Ar-H), 7.76 (s, 1H, CH═C), 7.95 (d, 1H, Ar-H, J = 8.28 Hz), 8.02 (d, 2H, Ar-H, J = 7.88 Hz), 8.80 (s, 1H, CH═N proton), 9.09 (s, 1H, pyrazole proton), 12.66 (br s, 1H, NH, D_2O exchangeable); ^{13}C NMR (DMSO-d_6): δ107.21, 111.43, 117.50, 119.82, 120.11, 121.48, 122.33, 123.76, 124.65, 125.52, 127.87, 128.09, 128.37, 128.60, 129.44, 130.46, 134.41, 139.22, 141.63, 148.45, 149.33, 151.27, 154.61, 175.73 (C═O). MS, *m/z* (%): 526, 524 [M^{+1}](16, 5), 76 [C_6H_4] (100). Anal. For$C_{28}H_{18}ClN_5O_2S$ (524.00): Calcd. C, 64.18; H, 3.46; N, 13.37; S, 6.12; Found: C, 64.26; H, 3.31; N, 13.19; S, 6.28.

5.1.2.13. 2-(((3-(Benzofuran-2-yl)-1-phenyl-1H-pyrazol-4-yl)methylene) hydrazono)-5-(2,4-dichlorobenzylidene)thiazolidin-4-one ***(16)***. Yield 77%, mp 229–230 °C, orange solid,IR (ν_{max}/cm^{-1}): 3128 (NH), 3047 (CH-aromatic),1709 (C═O), 1632 (C═N), 1595 (C═C).^{1}H NMR (DMSO-d_6): δ 7.31–7.32 (m, 1H, Ar-H), 7.38–7.47 (m, 4H, Ar-H), 7.57–7.61 (m, 2H, Ar-H), 7.65 (d, 1H, Ar-H, J = 7.36 Hz), 7.75 (d, 2H, Ar-H, J = 9.16 Hz), 7.81 (d, 1H, Ar-H, J = 8.44 Hz), 7.92 (s, 1H, CH═C proton), 8.04 (d, 2H, Ar-H, J = 7.92), 8.72 (s, 1H, CH═N proton), 8.99 (s, 1H, pyrazole proton) 12.52 (br s, 1H, NH, D_2O exchangeable); ^{13}C NMR (DMSO-d_6): δ107.45, 112.26, 117.62, 119.71, 120.24, 121.53, 121.91, 122.84, 124.14, 125.69, 127.91, 128.36, 128.74, 128.91, 129.56, 131.26, 134.68, 138.90, 141.15, 148.62, 149.14, 151.30, 154.82, 176.09 (C═O). MS, *m/z* (%): 557, 558, 559 [M$^+$] (19, 4, 7), 77 [C_6H_5] (100). Anal. For$C_{28}H_{17}Cl_2N_5O_2S$ (558.44): Calcd. C, 60.22; H, 3.07; N, 12.54; S, 5.74; Found: C, 60.38; H, 3.26; N, 12.33; S, 5.61.

5.1.2.14. 2-(((3-(Benzofuran-2-yl)-1-phenyl-1H-pyrazol-4-yl)methylene) hydrazono)-5-(4-bromobenzylidene)thiazolidin-4-one ***(17)***. Yield 93%, mp 249–251 °C, orange solid, IR (ν_{max}/cm^{-1}): 3132 (NH), 3063 (CH-aromatic), 1701 (C═O), 1628 (C═N), 1589 (C═C).^{1}H NMR (DMSO-d_6): 7.22 (s, 1H, Ar-H), 7.31–7.49 (m, 3H, Ar-H), 7.57–7.61 (m, 4H, Ar-H), 7.70–7.76 (m, 3H, Ar-H), 7.83–7.84 (m, 1H, Ar-H), 7.95–8.05 (m, 3H, CH═C, Ar-H), 8.71 (s, 1H, CH═N proton), 8.99 (s, 1H, pyrazole proton), 9.91 (s, 1H, NH, D_2O exchangeable); ^{13}C NMR (DMSO-d_6): δ106.97, 112.55, 117.02, 118.93, 119.69, 121.41, 121.97, 122.23, 122.82, 124.09, 125.42, 127.67, 128.40, 128.66, 128.97, 129.21, 131.5, 134.31, 141.15, 148.62, 149.14, 151.30, 154.82, 175.41 (C═O).MS, *m/z* (%): 568, 566 [M^{-1}] (100, 34). Anal. For$C_{28}H_{18}BrN_5O_2S$ (568.45): Calcd. C, 59.16; H, 3.19; N, 12.32; S, 5.64; Found: C, 59.25; H, 3.31; N, 12.08; S, 5.42.

5.1.2.15. 2-(((3-(Benzofuran-2-yl)-1-phenyl-1H-pyrazol-4-yl)methylene) hydrazono)-5-(naphthalen-1-ylmethylene)thiazolidin-4-one ***(18)***. Yield 82%, mp 283–284 °C, dark yellow solid,IR (ν_{max}/cm^{-1}): 3152 (NH), 3044 (CH-aromatic), 1705 (C═O), 1636 (C═N), 1597 (C═C).^{1}H NMR (DMSO-d_6): δ 7.29–7.44 (m, 3H, Ar-H), 7.54–7.72 (m, 7H, Ar-H), 7.84–7.89 (m, 2H, Ar-H), 8.00–8.07 (m, 4H, Ar-H), 8.15–8.19 (m, 2H, Ar-H, CH═C proton), 8.78 (s, 1H, CH═N proton), 9.08 (s, 1H, pyrazole proton), 11.18 (br s, 1H, NH, D_2O exchangeable), ^{13}C NMR (DMSO-d_6): δ 106.86, 112.35, 118.33, 118.82, 119.22, 119.36, 119.84, 121.54, 121.95, 122.11, 122.72, 123.61, 124.14, 125.23, 127.21, 128.11, 128.56, 128.84, 129.54, 130.34, 132.51, 133.67, 134.27, 135.07, 139.41, 141.62, 142.40, 149.33, 149.91, 154.44, 177.41 (C═O). MS, *m/z* (%): 539 [M$^+$] (45), 92 [C_7H_8] (100). Anal. For$C_{32}H_{21}N_5O_2S$ (539.61): Calcd. C, 71.23; H, 3.92; N, 12.98; S, 5.94; Found: C, 71.42; H, 3.71; N, 12.68; S, 5.80.

5.1.2.16. 2-(((3-(Benzofuran-2-yl)-1-phenyl-1H-pyrazol-4-yl)methylene) hydrazono)-5-(naphthalen-2-ylmethylene)thiazolidin-4-one ***(19)***. Yield 91%, mp 197–198 °C, yellow solid,IR (ν_{max}/cm^{-1}): 3159 (NH), 3051 (CH-aromatic), 1705 (C═O), 1628 (C═N), 1597 (C═C). ^{1}H NMR (DMSO-d_6): δ 7.28–7.45 (m, 4H, Ar-H), 7.53–7.67 (m, 4H, Ar-H), 7.72–7.98 (m, 6H, Ar-H), 8.05 (d, 2H, Ar-H, J = 8.52 Hz), 8.64 (s, 1H, Ar-H), 8.72 (s, 1H, CH═C proton), 9.05 (s, 1H, CH═N proton), 9.27 (s, 1H, pyrazole proton), 11.50 (s, 1H, NH, D_2O exchangeable);^{13}C NMR (DMSO-d_6): δ 107.32, 111.68, 118.45, 119.01, 119.25, 119.42, 121.84, 122.05, 122.69, 123.88, 124.05, 125.69, 127.09, 128.05, 128.43, 128.72, 130.21, 130.26, 132.69, 133.50, 134.10, 135.46, 139.21, 141.84, 142.58, 149.52, 149.78, 154.65, 178.11 (C═O). MS, *m/z* (%): 538 [M^{-1}] (29), 77 [C_6H_5] (100). Anal. For$C_{32}H_{21}N_5O_2S$ (539.61): Calcd. C, 71.23; H, 3.92; N, 12.98; S, 5.94; Found: C, 71.38; H, 3.64; N, 12.81; S, 5.76.

5.1.2.17. 2-(((3-(Benzofuran-2-yl)-1-phenyl-1H-pyrazol-4-yl)methylene) hydrazono)-5-((5-methylfuran-2-yl)methylene)thiazolidin-4-one ***(20)***. Yield 77%, mp 245–247 °C, yellow solid,IR (ν_{max}/cm^{-1}): 3125 (NH), 3059 (CH-aromatic), 1701 (C═O), 1632 (C═N), 1595 (C═C).^{1}H NMR (DMSO-d_6): δ 2.33 (s, 3H, CH_3), 6.35 (d, 1H, Ar-H, J = 2.48 Hz), 6.78 (d, 1H, Ar-H, J = 2.80 Hz), 7.22 (s, 1H, Ar-H), 7.31–7.45 (m, 3H, Ar-H), 7.58–7.62 (m, 2H, Ar-H), 7.72–7.75 (m, 2H, Ar-H), 7.90 (s, 1H, CH═C proton), 8.05 (d, 2H, Ar-H, J = 7.92), 8.76 (s, 1H, CH═N proton), 9.07 (s, 1H, pyrazole proton), 10.81 (br s, 1H, NH, D_2O exchangeable);^{13}C NMR (DMSO-d_6): δ 14.13, 107.17, 110.11, 111.77, 114.13, 117.05, 118.12, 119.51, 121.96, 123.86, 125.79, 127.96, 128.56, 130.21, 130.59, 139.14, 142.24, 148.06, 149.52, 149.65, 154.68, 155.75, 174.22 (C═O).MS, *m/z* (%): 493 [M$^+$] (21), 77 [C_6H_5] (100). Anal. For $C_{27}H_{19}N_5O_3S$ (493.54): Calcd. C, 65.71; H, 3.88; N, 14.19; S, 6.50; Found: C, 65.54; H, 3.62; N, 14.37; S, 6.29.

5.1.2.18. 2-(((3-(Benzofuran-2-yl)-1-phenyl-1H-pyrazol-4-yl)methylene) hydrazono)-5-(thiophen-2-ylmethylene)thiazolidin-4-one ***(21)***. Yield 65%, mp 240–242 °C, dark yellow solid,IR (ν_{max}/cm^{-1}): 3125 (NH), 3066 (CH-aromatic), 1700 (C═O), 1632 (C═N), 1591 (C═C). ^{1}H NMR (DMSO-d_6): δ 7.12 (s, 1H, Ar-H), 7.27–7.37 (m, 4H, Ar-H), 7.42 (s, 1H, Ar-H), 7.51–7.53 (m, 2H, Ar-H), 7.64–7.74 (m, 3H, Ar-H), 7.95–7.98

(m, 3H, CH═C, Ar-H),8.65 (s, 1H, CH═N proton), 8.93 (s, 1H, pyrazole proton), 11.12 (br s, 1H, NH, D_2O exchangeable);^{13}C NMR (DMSO-d_6): δ 107.16, 111.78, 115.42, 119.15, 119.43, 122.06, 123.76, 125.61, 127.72, 128.41, 128.66, 128.77, 129.57, 130.05, 130.17, 132.21, 139.33, 141.56, 141.82, 144.20, 149.90, 154.70, 179.73 (C═O). MS, *m/z* (%): 494 [M^{-1}] (26), 76 [C_6H_4] (100). Anal. For $C_{26}H_{17}N_5O_2S_2$ (495.58): Calcd. C, 63.01; H, 3.46; N, 14.13; S, 12.94; Found: C, 63.25; H, 3.31; N, 14.29; S, 12.68.

5.1.2.19. 2-(((3-(Benzofuran-2-yl)-1-phenyl-1H-pyrazol-4-yl)methylene) hydrazono)-5-(pyridin-4-ylmethylene)thiazolidin-4-one ***(22)***. Yield 61%, mp 248–250 °C, dark orange solid,IR (ν_{max}/cm^{-1}): 3125 (NH), 3048 (CH-aromatic),1710 (C═O), 1620 (C═N), 1598 (C═C).^{1}H NMR (DMSO-d_6): δ 7.20 (s, 1H, Ar-H), 7.33–7.44(m, 3H, Ar-H), 7.56–7.61 (m, 4H, Ar-H), 7.73–7.77 (m, 2H, Ar-H), 7.96 (s, 1H, CH═C), 8.05 (d, 2H, Ar-H, J = 7.88 Hz), 8.60 (d, 2H, Ar-H, J = 7.32 Hz), 8.75 (s, 1H, CH═N proton), 9.03 (s, 1H, pyrazole proton), 12.48 (br s, 1H, NH, D_2O exchangeable), ^{13}C NMR (DMSO-d_6): δ 107.24, 112.28, 116.07, 118.68, 119.22, 121.53, 122.84,122.51, 123.54, 124.92, 125.04, 127.43, 128.55, 129.64, 130.26, 139.41, 141.73, 144.36, 146.28, 148.20, 149.67, 155.06, 178.49 (C═O). MS, *m/z* (%): 491 [M^{+1}] (19), 64 [C_5H_4] (100).Anal. For$C_{27}H_{18}N_6O_2S$ (490.54): Calcd. C, 66.11; H, 3.70; N, 17.13; S, 6.54; Found: C, 66.24; H, 3.53; N, 17.24; S, 6.40.

5.2. Biological evaluation

5.2.1. In vitro anticancer activity

MTT assay was used to evaluate the *in vitro* cytotoxicity of the new compounds against cervix cancer cell lines Hela [21–23]. MTT assay depends on the reduction of the soluble 3-(4,5-methyl-2-thiazolyl)-2,5-diphenyl-2H-tetrazolium bromide (MTT) into a blue purple formazan product, mainly by mitochondrial reductase activity inside the living cells. The cells used in cytotoxicity assay were cultured in RPMI 1640 medium supplemented with 10% fetal calf serum. Cells suspended in the medium (2×10^4 cells/mL) were plated in 96-well culture plates and incubated at 37 °C in a 5% CO_2incubator. After 12 h, the test sample (2 μL) was added to the cells (2×10^4) in 96-well plates and cultured at 37∘C for 3 days. The cultured cells were mixed with 20 μL of MTT solution and incubated for 4 h at 37 °C. The supernatant was carefully removed from each well and 100 μL of DMSO were added to each well to dissolve the formazan crystals which were formed by the cellular reduction of MTT. After mixing with a mechanical plate mixer, the absorbance of each well was measured by a microplate reader using a test wavelength of 570 nm. The results were expressed as the IC50 (μM), which inducing a50% inhibition of cell growth of the treated cells when compared to the growth of control cells. Each experiment was performed at least 3 times. There was a good reproducibility between the replicate wells with standard errors.

5.2.2. In vitro radiometric EGFR kinase assay

Microliter plates were coated with 50 μL/well of the EGFR substrate ATF-2 (10 μg/mL in TBS) for 1.5 h at 37 °C. After washing three times with bidi stilled water, the remaining open binding sites were blocked with blocking buffer (BB; 0.05% Tween20 (Bio-Rad), 0.25% BSA, 0.02% NaN3 in TBS) for 30 min at room temperature. Plates were washed again, 50 μL of the respective test solution was filled into the wells, and the plates were incubated for1 h at 37 °C. Test solutions containing 12 ng/well p38 a MAPK were diluted in kinase buffer (50 mM Tris-HCl, pH 7.5, 10 mM MgCl2, 10 mM-Glycerophosphate, 100 μg/mL BSA, 1 μM Dithiothreitol, 0.1 mM Na_3VO_4, 100 μM rATP) with or without test substance (10–4–10–8 M). Test substances were dissolved in DMSO to form stock solutions of 10–2 M; all further dilution steps were carried out in kinase buffer. After subsequent washing, plates were blocked again with BB for 15 min followed by a fourth washing step. Wells were filled with 50 μL of the primary AB; Phospho-ATF-2 (Thr69/71)-Antibody (1:500 in BB) and incubated for 1 h at 37 °C of the secondary AB; Antirabbit IgG-AP-Antibody (alkaline phosphataseconjugated) (1:4000 in BB). Then 100 μL of 4-NPP (Nitrophenylphosphate)was pipetted in each well after a final washing step, and the color development was measured 1.5–2 h later with an enzyme-linked immunosorbent assay reader linked equipped with SOFT max PRO software at 405 nm [34].

5.2.3. Cell cycle analysis and apoptosis detection

Cell cycle analysis and apoptosis investigation were carried out by flow cytometry [35]. MCF-7 cells were seeded at 8×10^4 and incubated at 37 °C, 5% CO_2 overnight. After treatment with thetested compound, for 24 h, cell pellets were collected and centrifuged (300*g*, 5 min). For cell cycle analysis, cell pellets were fixed with 70% ethanol on ice for 15 min and collected again. The collected pellets were incubated with propidium iodide (PI) staining solution (50 mg/mL PI, 0.1 mg/mL RNaseA, 0.05% Triton X-100) at room temperature for 1 hand analyzed by Gallios flow cytometer (Beckman Coulter, Brea, CA, USA). Apoptosis detection was performed by FITC Annexin V/PI commercial kit (Becton Dickenson, Franklin Lakes, NJ, USA) following the manufacture protocol. The samples were analyzed by fluorescence-activated cell sorting (FACS) with a Gallios flow cytometer (Beckman Coulter, Brea, CA,USA) within 1 h after staining. Data were analyzed using Kaluzav 1.2 (Beckman Coulter).

5.2.4. Measurement of the effect of compound 14 on the level of p53, Baxand BCL-2

The levels of the tumor suppressor gene p53, anti-apoptotic markerBCL-2 as well as the apoptotic marker Bax were assessed using BIO RAD iScript TM One-Step RT-PCR kit with SYBR® Green. The procedure of the used kit was done according to the manufacturer's instructions [36].

5.2.5. Caspases-3, -7 assays

Activities of caspases-3, -7 were measured using DRG Caspase-3 (human) ELISA (EIA-4860) kit (DRG International Inc., USA), Invitrogen. Caspase-7 (Active) (human) ELISA kit, Catalog # KHO1091 (96 tests) (Invitrogen Corporation, USA) according to the manufacturer instructions.

5.3. Molecular docking study

The X-ray crystallographic structure of Epidermal Growth Factor Receptor (EGFR) co-crystallized with the 4-anilinoquinazoline derivative erlotinib (PDB ID: 1M17) was downloaded from the protein data bank [32,33]. Water molecules and ligands that are not involved in binding were removed. Then, the protein was prepared for docking study using Protonate 3D protocol in MOE with default options. The co-crystalized ligand was used to define the binding site for docking. The co-crystalized ligand was used to define the binding site for docking. Triangle Matcher placement method and London dG scoring function were used for docking. Docking setup was first validated by re-docking of the co-crystallized ligand (erlotinib) in the vicinity of the binding site of the enzyme with energy score (S) = −11.08 kcal/mol and RMSD of 1.321 Å and with the ability to reproduce all the key interactions accomplished by the co-crystallized ligand with the key amino acids in the binding site. The validated docking protocol was then used to study the ligand-target interactions in the active site for the most potent compound **14** to predict its binding mode to rationalize its promising activity.

Acknowledgments

The authors extend their appreciation to the Deanship of Scientific Research at King Khalid University for funding this work through General Research Project under Grant number (G.R.P 258-39) and thanking to Dr. Essam Rashwan, head of confirmatory diagnostic unit,

Vacsera-Egypt, for helping in performing the biological screening. Also, thanking to Dr. Ahmed M. El Kerdawy, Molecular Modeling Unit, Faculty of Pharmacy, Cairo University, Kasr El-Aini Street, Cairo, Egypt, for performing molecular docking study.

References

[1] Y.A. Ammar, A.M. Sh El-Sharief, A. Belal, S.Y. Abbas, Y.A. Mohamed, A.B.M. Mehany, A. Ragab, Design, synthesis, antiproliferative activity, molecular docking and cell cycle analysis of some novel (morpholinosulfonyl) isatins with potential EGFR inhibitory activity, Eur. J. Med. Chem. 156 (2018) 918–932.
[2] World Health Organisation, 'Cancer' (accessed 31 January 2019) < http://www.who.int/cancer/en > .
[3] World Health Organisation, Cervical cancer < https://www.who.int/cancer/prevention/diagnosis-screening/cervical-cancer/en > .
[4] P. Li, Y. Tian, H. Zhai, F. Deng, M. Xie, X. Zhang, Studies on the inhibitory models of pyrazoline derivatives as EGFR kinase inhibitors by 3D-QSAR and molecular docking, Med. Chem. Res. 23 (2014) 2869–2879.
[5] J.R. Woodburn, The epidermal growth factor receptor and its inhibition in cancer therapy, Pharmacol. Ther. 82 (1999) 241–250.
[6] Y. Tu, C. Wang, S. Xu, Z. Lan, W. Li, J. Han, Y. Zhou, P. Zheng, W. Zhu, Design, synthesis, and docking studies of quinazoline analogues bearing aryl semicarbazone scaffolds as potent EGFR inhibitors, Bioorg. Med. Chem. 25 (2017) 3148–3157.
[7] Hai-Chao Wang, Xiao-Qiang Yan, Tian-Long Yan, Hong-Xia Li, Zhong-Chang Wang, Hai-Liang Zhu, Design, synthesis and biological evaluation of benzohydrazide derivatives containing dihydropyrazoles as potential EGFR kinase inhibitors, Molecules 21 (2016) 1012.
[8] P. Cohen, D.R. Alessi, Kinase drug discovery–what's next in the field? ACS Chem. Biol. 8 (2013) 96–104.
[9] S. Knapp, M. Sundström, Recently targeted kinases and their inhibitors – the path to clinical trials, Curr. Opin. Pharmacol. 17 (2014) 58–63.
[10] D. Fabbro, 25 years of small molecular weight kinase inhibitors: potentials and limitations, Mol. Pharmacol. 87 (2015) 766–775.
[11] F.M. Ferguson, N.S. Gray, Kinase inhibitors: the road ahead, Nat. Rev. Drug Discov. 17 (2018) 353–377.
[12] P. Wu, T.E. Nielsen, M.H. Clausen, Small-molecule kinase inhibitors: an analysis of FDA-approved drugs, Drug Discov. Today 2 (2016) 5–10.
[13] A. Carella, V. Roviello, R. Iannitti, R. Palumbo, S. La Manna, D. Marasco, M. Trifuoggi, R. Diana, G.N. Roviello, Evaluating the biological properties of synthetic 4-nitrophenyl functionalized benzofuran derivatives with telomeric DNA binding and antiproliferative activities, Int. J. Biol. Macromol. 121 (2019) 77–88.
[14] F. Xie, H. Zhu, H. Zhang, Q. Lang, L. Tang, Q. Huang, L. Yu, *In vitro* and *in vivo* characterization of a benzofuran derivative, a potential anticancer agent, as a novel Aurora B kinase inhibitor, Eur. J. Med. Chem. 89 (2015) 310–319.
[15] Md. Jawaid Akhtar, A.A. Khan, Z. Ali, R.P. Dewangan, Md. Rafi, Md. Quamrul Hassan, Md. Sayeed Akhtar, A.A. Siddiqui, S. Partap, S. Pasha, M. ShaharYar, Synthesis of stable benzimidazole derivatives bearing pyrazole as anticancer and EGFR receptor inhibitors, Bioorg. Chem. 78 (2018) 158–169.
[16] S.S. Abd El-Karim, Y.M. Syam, A.M. El Kerdawy, T.M. Abdelghany, New thiazol-hydrazono-coumarin hybrids targeting human cervical cancer cells: synthesis, CDK2 inhibition, QSAR and molecular docking studies, Bioorg. Chem.86 (2019) 80–96.
[17] S. Thakral, D. Saini, A. Kumar, N. Jain, S. Jain, A synthetic approach and molecular docking study of hybrids of quinazolin-4-ones and thiazolidin-4-ones as anticancer agents, Med. Chem. Res. 26 (2017) 1595–1604.
[18] M. Bhat, B. Poojary, B.S. Kalal, P.M.G. Swamy, S. Kabilan, V. Kumar, N. Shruthi, S.A.A. Anand, V.R. Pai, Synthesis and evaluation of thiazolidinone–pyrazole conjugates as anticancer and antimicrobial agents, Future Med. Chem. 10 (2018) 1017–1036.
[19] H. Taniguchi, T. Yamada, R. Wang, et al., AXL confers intrinsic resistance to osimertinib and advances the emergence of tolerant cells, Nat. Commun. 10 (2019) 259.
[20] M.I. El-Zahar, S.S. Abd El-Karim, M.M. Anwar, Synthesis and cytotoxicity screening of some novel benzofuranoyl-pyrazole derivatives against liver and cervix carcinoma cell lines, S. Afr. J. Chem. 62 (2009) 189–199.
[21] Kamelia M. Amin, Yasmin M. Syam, Manal M. Anwar, Hamed I. Ali, Tamer M. Abdel-Ghani, Aya M. Serry, Synthesis and molecular docking study of new benzofuran and furo[3,2-g]chromone-based cytotoxic agents against breast cancer and p38α MAP kinase inhibitors, Bioorg. Chem. 76 (2018) 487–500.
[22] Kamelia M. Amin, Yasmin M. Syam, Manal M. Anwar, Hamed I. Ali, Tamer M. Abdel-Ghani, Aya M. Serry, Synthesis and molecular docking studies of new furochromone derivatives as p38a MAPK inhibitors targeting human breast cancer MCF-7 cells, Bioorg. Med. Chem. 25 (2017) 2423–2436.
[23] G. Thiessen, H. Thiessen, Microspectrophotometric cell analysis, Prog. Histochem. Cytochem. 9 (1977) 1–156.
[24] M.S.A. Elsayed, M.E. El-Araby, R.A.T. Serya, A.H. El-Khatib, M.W. Linscheid, K.A.M. Abouzid, Structure-based design and synthesis of novel pseudosaccharine derivatives as antiproliferative agents and kinase inhibitors, Eur. J. Med. Chem. 61 (2013) 122–131.
[25] G. Luo, Z. Tang, K. Lao, X. Li, Q. You, H. Xiang, Structure-activity relationships of 2,4-disubstituted pyrimidines as dual ERa/VEGFR-2 ligands with activity, Eur. J. Med. Chem. 150 (2018) 783–795.
[26] M.A. Aziz, R.A.T. Serya, D.S. Lasheen, A.K. Abdel-Aziz, A. Esmat, A.M. Mansour, A.B. Singab, K.A.M. Abouzid, Discovery of potent VEGFR-2 inhibitors based on furopyrimidine and thienopyrimidne scaffolds as cancer targeting agents, Sci. Rep. 6 (2016) 24460, https://doi.org/10.1038/srep24460.
[27] F. Liu, D. Liu, Y. Yang, S. Zhao, Effect of autophagy inhibition on chemotherapy-induced apoptosis in A549 lung cancer cells, Oncol Lett. 5 (2013) 1261–1265.
[28] K.C. Zimmermann, D.R. Green, How cells die: apoptosis pathways, J. Aller. Clin. Immunol. 108 (4 Suppl.) (2001) S99–S103.
[29] A. Frenzel, F. Grespi, W. Chmelewskij, A. Villunger, Bcl2 family proteins in carcinogenesis and the treatment of cancer, Apoptosis 14 (2009) 584–596.
[30] T. Miyashita, S. Krajewski, M. Krajewska, H.G. Wang, H.K. Lin, D.A. Liebermann, B. Hoffman, J.C. Reed, Tumor suppressor p53 is a regulator of bcl-2 and bax gene expression in vitro and in vivo, Oncogene 9 (1994) 1799–1805.
[31] D.W. Nicholson, P. Nicotera, G. Melino, Caspases and Cell Death, Encyclopedia of Biological Chemistry, first ed., Elsevier, 2004, pp. 319–327.
[32] http://www.rcsb.org/.
[33] J. Stamos, M.X. Sliwkowski, C. Eigenbrot, Structure of the epidermal growth factor receptor kinase domain alone and in complex with a 4-anilinoquinazoline inhibitor, J. Biol. Chem. 277 (2002) 46265–46272.
[34] H.-L. Qin, J. Leng, B.G.M. Youssif, M.W. Amjad, M.A. Raja, M.A. Hussain, Z. Hussain, S.N. Kazmi, S.N.A. Bukhari, Synthesis and mechanistic studies of curcumin analog-based oximes as potential anticancer agents, Chem. Biol. Drug Des. 90 (2017) 443–449.
[35] S. Diab, T. Teo, M. Kumarasiri, P. Li, M. Yu, F. Lam, S.K.C. Basnet, M.J. Sykes, H. Albrecht, R. Milne, S. Wang, Discovery of 5-(2-(phenylamino)pyrimidin-4-yl) thiazol-2(3H)-one derivatives as potent Mnk2 inhibitors: synthesis, SAR analysis and biological evaluation, Chem. Med. Chem. 9 (2014) 962–972.
[36] E.F. Abdelhaleem, M.K. Abdelhameid, A.E. Kassab, M.M. Kandeel, Design and synthesis of thienopyrimidine urea derivatives with potential cytotoxic and proapoptotic activity against breast cancer cell line MCF-7, Eur. J. Med. Chem. 143 (2018) 1807–1825.